Water at solid surfaces: A review of selected theoretical aspects and experiments on the subject

M. Maccarini[a)]
Angewandte Physikalische Chemie, Ruprecht Karls Universität Heidelberg, Im Neunheimer Feld 253, 69120 Heidelberg, Germany

(Received 12 September 2006; accepted 12 July 2007; published 21 August 2007)

This review summarizes select aspects of the research on solid/water interfaces. Despite the considerable amount of work, the way water molecules are organized at the interface is still a source of debate. Theoretical efforts will be presented in combination with the results of computer simulations. The current status of investigations obtained with x-rays and neutron reflectometries, and sum frequency generation spectroscopy (all sensitive to the properties of solid/liquid interfaces) will be summarized and discussed. © *2007 American Vacuum Society.* [DOI: 10.1116/1.2768902]

I. INTRODUCTION

The properties of a liquid close to a solid surface are distinctly different from those in the bulk.[1–3] The attractive/repulsive interactions between a substrate surface and liquid molecules, as well as the geometric constraint by the solid surface, cause structural changes that extend into the bulk liquid over the so-called solvation (or, for water, hydration) layer. [The decay of the surface-induced structural changes in the liquid is described in the theory of solvation by exponential or inverse power law functions of distance (see, for example, Ref. 4). Thus, a specific criterion should be used to define the boundary between the solvation layer and the bulk liquid. This is, however, outside the scope of this review and hereafter the solvation layer will be generically referred to as the layer of liquid molecules, which are significantly affected by the presence of the solid surface.] While at large distances the interactions between two surfaces can be described in terms of electrostatic and van der Waals interaction, which regard the fluid between them as a continuum, at distances comparable to a few molecular diameters, the discrete nature of the solvent emerges and the forces between the surfaces differ from those predicted by the continuum theories. Thus, solvation forces, associated with the surface-induced structural changes in the liquid, arise as the surfaces approach each other.

The solid/fluid interaction can lead to ordering into molecular layers parallel to the surface. This results in decaying oscillations of the one-body fluid density profile, with a periodicity determined by the diameter of the fluid molecules.[5] When the solvation layers of the two objects overlap, the fluid density oscillations propagating from the opposite surfaces may interfere constructively or destructively, leading to attractive or repulsive solvation forces between the two objects. Also possible is transversal ordering by the presence of an atomically structured surface,[5–7] which, under some conditions, can act like a template for the adjacent fluid layer. Orientational ordering induced by solid surfaces has been observed for n-alkanes, which are preferentially adsorbed with their molecular axis parallel to the confining surfaces,[8] and is predicted for water near hard and nonorienting walls (i.e., even when the surface-fluid interaction potential is independent of the orientation).[9,10] Any molecular orientation of the liquid molecules induced by a substrate will inhibit their ability to interact with neighboring liquid molecules as in the bulk fluid, and thus may result in a different liquid density at the interface as compared to the bulk liquid. This density difference at the solid/fluid interface is one important factor that determines the sign and the magnitude the solvation forces (hydration forces for water) between immersed objects, along with other factors like the type of ordering and the interactions between the liquid and the surface. Thus, the understanding of the relation between these factors and the resulting hydration forces is of fundamental importance in colloid science[2] and biology.[11]

This review will summarize the present theoretical understanding and experimental data for water interaction with non-ionic surfaces as encountered in technological applications and omnipresent in biological interphases. In the experimental part we focus on neutron and x-ray scattering and sum frequency generation (SFG) spectroscopy experiments, which probe the density and the structure of the H bond network at the water/solid interphase. Although the inclusion of a detailed discussion on surface-force experiments would be a natural follow-up to the theoretical and the experimental part, we do not intend to review the numerous surface-force and AFM experiments on hydration interactions for two reasons: first, an outstanding review was already published by Christenson and Claesson.[12] Second, the wide body of surface-force measurement gives results that are difficult to rationalize and, in many cases, contradicting. On one hand, the lack of a proper characterization prior and subsequent to the measurement affects the reliability of the published measurement.[12] On the other hand, the contribution to the surface-force of unavoidable defects present on the surface becomes more and more relevant as the two surfaces get closer. At distances of a few nanometers, they can drastically affect the force measurement.[2]

The behavior of water at softer surfaces like lipid membranes is outside the scope of this review, but many aspects

[a)]Present address: Institut Laue-Langevin, 6, rue Jules Horowitz, BP 156 - 38042 Grenoble Cedex 9, France; electronic mail: maccarini@ill.fr

(e.g., hydrophobicity/hydrophilicity, hydrogen bonding, water orientation, hydration, etc.) apply equally to these systems. The interested reader can find the topic discussed in two very interesting reviews[13,14] and other computational works.[15–17]

II. THEORETICAL CONSIDERATIONS OF WATER/SOLID INTERACTIONS

A. Hydrophilicity and hydrophobicity

The terms hydrophilic and hydrophobic are commonly used to describe the nature of water interaction with surfaces, colloidal particles, or solutes. Intuitively, hydrophilic (hydrophobic) objects attract water molecules more (less) strongly than water molecules attract one another, and a hydrophobic (hydrophilic) surface is a surface capable (incapable) of strong hydrogen bonding with water. However, the interaction of surfaces with water is not simply related to the number or strength of hydrogen bonds, but depends on various factors such as the rigidity of the surface groups able to form H-bonds and how they are distributed on the surface (e.g., areal density and lateral arrangement).[10] Therefore, the water affinity of a surface cannot be expressed in terms of a single factor.

From the thermodynamical point of view, the affinity between a surface and water is expressed in terms of water-surface interfacial tension, γ_{ws}. When this quantity is negative (positive), i.e., increasing (decreasing) the water-surface interface lowers the energy of the system, the surface is hydrophilic (hydrophobic). By means of the Young equation, $\gamma_{wv}\cos(\theta)=\gamma_{sv}-\gamma_{ws}$, where the subscript v indicates water vapor, the water-surface interfacial tension, γ_{ws}, relates to the contact angle, θ. It is often assumed that the change over from hydrophobic to hydrophilic behavior occurs at a contact angle of $\theta=90°$ where $\gamma_{ws}=\gamma_{sv}$. Since the contact angle when $\gamma_{ws}=0$ depends also on the solid/vapor interfacial tension, γ_{sv},[10,18] which is always positive, the change over from hydrophobic to hydrophilic behavior depends on the substrate material and not only on the measured water/solid contact angle. The contact angle is a practical criteria to determine the wettability of a solid by a liquid. Its determination is subject, however, to some difficulties arising from the pinning of the contact line (the line that in the situation of partial wetting delimits the wetted portion of the surface) on surface defects, resulting in hysteresis in the contact angle measured as the solid/liquid surface increases (advancing contact angle) or decreases (receding contact angle). Roughness, for instance, causes the surface to have discontinuities in the slope that induce fluctuation in the contact angle,[19] as was shown by Dettre and Johnson with contact angle measurements at increasing roughness.[20] Theoretical models to describe how the contact line is pinned between subsequent grooves on a surface are described in a seminal review on wetting[21] of periodic surfaces and surfaces with random fluctuation in shape. Contact angle hysteresis can be due also to surface contamination, and to the presence of solutes in the liquid that in some circumstances can form a film on the surface.

A definition for hydrophobicity and hydrophilicity, independent of the nature of the solute or solid, can be derived from the sign of the hydration pressure, p_h, between two parallel surfaces immersed in water at a distance H, $p_h=-(\partial\gamma/\partial H)_{\mu,T}$. γ denotes the tension of a water film confined between the two surfaces, which depends on the distance H. For $H\to\infty$ we have that $\gamma_{ws}=\gamma(H)/2$. Provided that the distance H between the two surfaces is large enough that the hydration pressure is a monotonic function of this parameter, the hydrophilicity (hydrophobicity) criterion based on the water-surface interfacial tension is equivalent to the condition that p_h is repulsive (attractive). The hydrophilicity/hydrophobicity criterion based on the contact angle overestimates the hydrophilicity of a surface compared to the p_h-based criterion, i.e., in the interval $0<\gamma_{wv}\cos(\theta)<\gamma_{sv}$, according to the contact angle criterion, the surface is hydrophilic, whereas following the p_h-based criterion the surface is still hydrophobic. The offset between the two hydrophilicity/hydrophobicity criteria is elaborated in Vogler's review,[18] where he evaluated the characteristic decay length of the force between partially silanized surfaces as a function of the contact angle. The crossover between attractive and repulsive characters of the force occurs at a contact angle of $\theta\sim 62$ deg. Thus, the region between 62 and 90 deg is hydrophilic, according to the contact angle criterion, and hydrophobic, according to the hydration pressure criterion. In this article, these terms will be used only when there is no ambiguity, i.e., for surfaces whose contact angle is well below 62 deg or higher than 90 deg.

B. Thermodynamics of liquids confined between solid surfaces

The density and molecular arrangement in confined fluids and the resulting solvation forces have been the subject of many theoretical studies. The basic thermodynamics was described by Ash *et al.*[22] and Hall[23] and subsequently elaborated by Evans *et al.*:[1] with reference to Fig. 1, we consider two parallel surfaces of surface area A, immersed in a volume V of fluid. The two plates are subject to external forces f, which keep them at separation distance H. The system is described by the grand canonical ensemble (i.e., at constant μVT) in order to account for the experimental condition of an open system (i.e., exchange of molecules between the bulk and confined liquid). The grand potential function is $\Omega=U-TS-\mu N$. If we denote with Ω_0 the grand potential that the system would have without the surfaces, we define with $\Omega'=\Omega-\Omega_0$ the excess grand potential. It results that $\Omega'=2A\gamma$, where 2γ is the surface tension of the water film between the plates. Ω' and γ depend on the separation H. For $H\to\infty$, γ is equal to the fluid-surface interfacial tension, whereas at $H=0$, the difference between the system with and without plates disappears and consequently $\Omega'(0)=\gamma(0)=0$. If p_h is the solvation pressure between the surfaces, the following relationships hold:

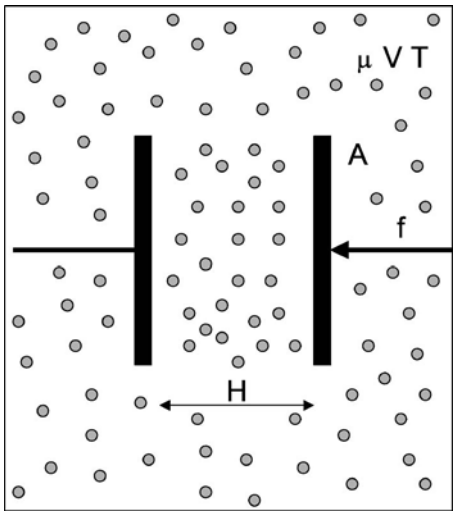

FIG. 1. System of two parallel plates of area A immersed in water. p_h is the solvation pressure between the surfaces and $f=p_aA$ is the external force applied to keep the surfaces at a given separation H.

$$p_h = \frac{1}{A}\left(\frac{\partial \Omega'}{\partial H}\right)_{\mu,T} = -2\left(\frac{\partial \gamma}{\partial H}\right)_{\mu,T}, \tag{1}$$

$$\gamma(H) = \frac{1}{2A}\Omega'(H) = -\frac{1}{2}\int_0^H p^h dH'. \tag{2}$$

The general correlation between the layering of the liquid structure and the resulting solvation pressure was determined by Attard *et al.*[24] They provided a description of the free energy per unit area between planar walls for a dense fluid. For hard spheres confined between hard walls, they predicted a decaying oscillatory solvation pressure with a period slightly greater than the liquid hard-sphere diameter. The oscillations asymptotically converged to the bulk pressure of the fluid. A dipolar moment was added to the hard spheres in order to elucidate the behavior of dipolar fluids: for smaller separations the pressure was qualitatively similar to the one observed for nonpolar fluids, but for large separations an attractive pressure was found, in contrast to the nonpolar fluid.

The decay of the density oscillations in the liquid structure was studied in detail by Evans *et al.*[4] In this work, the universal character of decay was pointed out, for a model fluid characterized by short-range interaction. Evans *et al.* identified two classes of decay: a monotonic exponential decay and an exponentially damped oscillatory decay. The first kind occurs generally at low temperature and density. High-density liquids are associated with damped oscillations of the liquid structure. The crossover between the two regimes defines a line in the (ρ,T) plane known as the Fisher-Widom line.

Understanding solvation phenomena in water, i.e., hydration phenomena, presents several difficulties: despite the simple chemical structure, the phase behavior of water is very complex due to the fact that every molecule has two proton donors and two acceptors, leading to a strong network of hydrogen bridge-bonded water. The presence of a discontinuity (such as a hard wall) not only induces changes in local density as compared to the bulk fluid, but also affects the orientational distribution of molecules and, hence, the hydrogen-bond network and density in the adjacent liquid-water layers. A further difficulty arises from the fact that H-bonding is a colligative phenomenon.

How the density in water changes in the presence of solutes was studied by Lum *et al.*,[25] who developed a unified theory to describe the solvation of small and large nonpolar species in water. Small nonpolar solutes have a low solubility in water due to the fact that they can be fitted in the clathrate cage formed by neighboring water molecules without the loss of too many H-bonds. Larger hydrophobes disrupt the network of hydrogen bonding, which can result in instability phenomena and drying. The crossover between the two regimes occurs at length-scales of the order of nanometers. Since the introduction of a hydrophobic body into water expels fluid molecules, the theory develops a general treatment of the excluded volume effect. [The excluded volume effect arises from the fact that two molecules cannot occupy the same space at the same time. Therefore, molecules induce with their presence an effective interaction on neighbors that prevents them from occupying sites already taken by other molecules.] The solute-water radial distribution function, $g(R+r)$, is analyzed as a function of the radius R of a hard sphere immersed in water. At small radii R, g presents oscillations due to the granularity of the fluid. In this regime structuring of water around the hydrophobic object is still possible, so that a hydration shell with clathrate geometry surrounds the solute, increasing the density of water close to it. At larger R (>1 nm), a depletion of the water density is predicted. For two parallel hydrophobic plates, a region of water thermodynamically less stable than a vapor phase is predicted for plate separations smaller than ~ 5 nm, leading to instability of the liquid and cavitation. In this context, several surface-force measurements of hydrophobic plates in water can be interpreted, in which a long-range attractive force and (at smaller separation) jump-into-contact were observed. The work of Lum shows quite clearly that hydration phenomena have a pronounced dependence on the radius of curvature of the surface in contact with water. Consequently, the microscopic roughness of a surface is expected to play an important role in the interpretation of solvation forces.

The role of molecular orientation of water on the interaction with surfaces was studied by Besseling.[26] He provided a statistical thermodynamic model based on a lattice-fluid theory of water. Surfaces carrying equal amounts of donors and acceptors and surfaces that only present hydrogen bonding donor sites were considered. His results show that there is not a simple correlation between the affinity of surfaces to water and the surface-forces resulting for confining water between two surfaces. Although it is generally excepted that highly hydrophobic surfaces show attractive interaction in water due to the prevalence of the density effect, for more hydrophilic surfaces both attraction or repulsion can occur,

depending on the relative contribution of density and orientational effects. When a surface affects the orientational ordering of water molecules, then the solvation layer propagating from opposite surfaces can cause disruption of such order and induction of attractive surface-forces, even in hydrophilic surfaces. However, density effects are generally more relevant than orientational, so it is common to observe attraction between hydrophobic surfaces in water and repulsion between hydrophilic ones.[26]

C. Computer simulations

Detailed information on the molecular origin of solvation forces has been obtained by means of computer simulations, which allow the reproduction of the structure of the confined fluid and the correlation of this with the solvation forces. Most of these studies are concerned with simple Lennard-Jones fluids and the confining walls are either assumed to be smooth or are represented by force centers arranged in face-centered cubic 100 or 111 lattices.[6,7,27,28] These simulations give detailed insight on the interrelation between fluid density in the confined space and the resulting solvation forces. For water, the simulations are more difficult because the complexity of hydrogen bridge bonding in water and its collective nature cannot be explicitly described by two body potentials.[29] However, the most important properties of water, including the anomaly in the temperature dependence of its density, can adequately be represented by two-body potential, when they are parameterized in a way that reproduces some selected properties of the liquid. Thus, they reflect, in an effective way, the collective phenomena in water, even though the potentials do not include any explicit many-body terms. In the last years, few explicit many-body water models have became available for computer simulations.[30]

Molecular dynamic (MD) computer simulations were used by Wallqvist and Berne[31] to study the hydration force between two hydrophobic ellipsoidal plates immersed in water. The interactions between water molecules were modeled by a reduced effective representation (RER)[32] developed to describe a liquid with highly directional hydrogen bonds in a tetrahedral network, and a purely repulsive inverse-power potential was used to account for the water-plate interactions. As the separation between the two ellipsoids was reduced, a weak oscillating force was observed, corresponding to the removal of water layers. When the distance was so small that only two layers could fit between the ellipsoid, a further approach led to a dewetting transition and subsequent strong attraction between the ellipsoids.

No dewetting transition was instead found in other isotension ensemble Monte Carlo (MC) simulations performed by Forsman *et al.*[33] on water confined between hard walls. The simple point charge (SPC) model[34] of water was used to describe the water interaction and the wall was considered hard only with respect to the oxygen atom. A strong attraction between the walls was observed, caused by density depression of the liquid between them.

Although the H-bond is highly directional, the water-wall potential employed in the simulation described above was independent of the orientation of the water molecule with respect to the wall. The influence of the orientation of the water-wall potential on the hydration force was studied by Hayashi *et al.*[10] with grand canonical Monte Carlo (GCMC) simulations. The TIP4P[35] model potential was used to describe the water-water interactions. The water-wall potential was taken as an inverse (9-3) power function, where the contribution of the two water protons and the lone electron pairs was assumed to depend on their orientation relative to the wall. By doing this, walls containing only proton acceptors, donors, or both could be considered by simply including or excluding the contributions due to the proton acceptors and/or lone electron pairs. In agreement with the theoretical studies of Besseling,[26] the simulation showed that attraction between hydrophilic walls may be possible due to the orientational ordering induced by the surfaces on the adjacent water layers. As a matter of fact, the model potential used to describe the water-wall interaction included a contribution related to the flexibility of the surface group involved in the hydrogen bonding, i.e., their ability to adapt their orientation to the approaching water molecule; rigid surface groups hinder this ability, resulting in unfavorable energy contributions, which make the surface less hydrophilic. For hydrophobic surfaces, two different types of attractions were found: at separation greater than ~ 6 nm, attraction was a consequence of water density depletion. At smaller separation, it was due to capillary evaporation of the confined water. On the contrary, Forsman *et al.*[36] did not observe attractive interactions between hydrophilic walls. This could be a result of the different analytical form of the orienting terms.

The theoretical predictions of Lum *et al.*[25] are supported by recent MD simulations[37] in which the density profile of water close to spherical and planar hydrophobic surfaces (simulated by a single-spherical solute with a varying radius inside a cubic box filled with SPC water or a planar hydrophobic substrate formed by a layer of parallel alkane molecules oriented normal to the interface) was studied (Fig. 2). For planar surfaces, a layer of reduced water density (depletion layer) was predicted. The simulations were aimed at elucidating the dependence on the radius of curvature, pressure, and temperature of this layer. The results are expressed and analyzed in terms of the depletion distance d_2 (Ref. 37) defined as

$$d_2 = \int dz \left(1 - \frac{\rho_{hc}(z)}{\rho_{hc,\mathrm{bulk}}} - \frac{\rho_w(z)}{\rho_{w,\mathrm{bulk}}} \right), \tag{3}$$

where ρ indicates the density and the indices hc and w refer to hydrocarbon and water, respectively. The depletion distance, d_2, should not be confused with the thickness of the depletion layer, which is related to the extension of the density gradient from the surface. It corresponds to the integral difference between the actual density across the interface and the corresponding bulk densities on both sides of the interface normalized to unity. This parameter is a way to quantify the density-depletion layer so that a meaningful comparison between theoretical studies and experiments can be attempted.

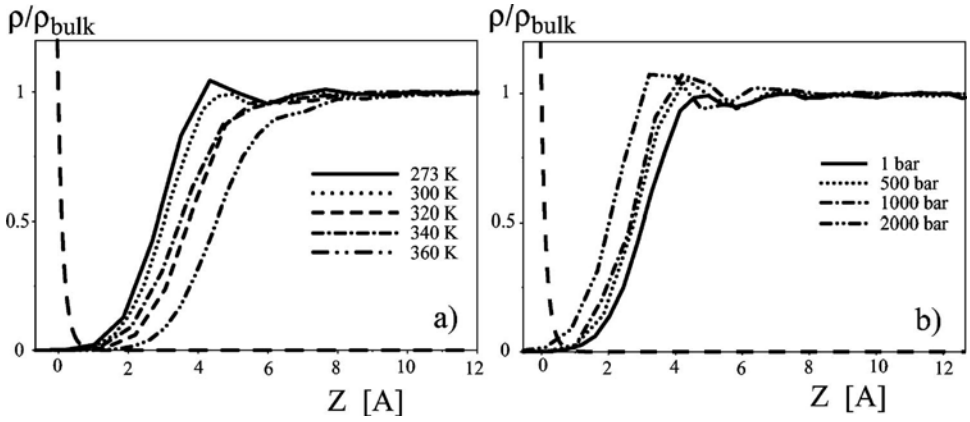

FIG. 2. (a) Temperature dependence of the water density profile close to a planar hydrophobic wall at fixed pressure $p=1$ bar. The Lennard-Jones potential of the hydrophobic layer is denoted by a broken line (to the left). (b) Pressure dependence of the water profile for fixed temperature $T=300$ K. In all cases, the simulation box contained 64 hydrophobic molecules and 2781 SPC/E water molecules. The system was thermalized for 100 ps and averaged for 2 ns. The figure is reproduced with permission from Ref. 37.

Netz and co-workers showed that increasing the radius of curvature of the hydrophobic surface decreases the depletion length of the layer. While the properties of this layer were found to be relatively insensitive to pressure, a dependence on temperature was found. Increasing temperature increases the thickness of the depletion layer. The simulations gave a value of d_2 ranging from 0.21 nm at a temperature of 273 K to 0.29 nm at 360 K. The simulation also predicted the presence of a large electrostatic surface potential (about +0.5 V) due to the strong orientation of the interfacial water molecules, which tends to orient their hydrogen atoms and thus their dipole toward the hydrophobic surface. Other GCMC simulations predict the opposite orientation of the water molecules confined between graphite sheets.[38] The principal objective of this study was to explain the well-known effect of environmental humidity on the friction and wear of graphitic carbons. Three different water-graphite model potentials were tested and it was shown that the thermodynamic and structural properties of the confined water are very sensitive to the range and to the orientational dependence of the model potential. This raises doubts concerning the results of previous simulations using orientation-independent potentials, which predicted an unusual behavior of water inside carbon nanotubes.[39–41]

Pertsin and Grunze[42] performed GCMC simulations of water confined in asymmetric slitlike nanopores formed by two parallel walls, one hydrophilic and one hydrophobic. The simulations were done in the presence of structureless nonorienting, as well as structured orienting, walls. It was found that when the density-corrected excess-chemical potential of the liquid μ'' was set slightly above the value at the liquid-vapor coexistence, $\mu''_{sat} \sim -6.2$ kcal mol^{-1}, the system was characterized by very large fluctuations of the number of water molecules and a wandering liquid-vapor interface. The importance of this study is twofold. On one hand, the simulation was in agreement with recent surface-force-apparatus experiments performed on water in a similar asymmetric confinement,[43] the so-called Janus interface. These experiments revealed a very noisy response of the system. On the other hand, a region with reduced density with a clear dependence on the excess chemical potential was found near the hydrophobic surface. The extension of such region increases as the μ'' approaches the liquid-vapor coexistence value (see Fig. 3).

GCMC simulations were performed on surfaces formed by oligo (ethyleneglycol) (OEG)-terminated alkanethiol[44] adsorbed on gold and silver. The interaction of these monolayers measured with scanning force microscope depend strongly on the substrate on which they are adsorbed. OEG-modified gold surfaces repel each other in electrolyte solutions and they are resistant to protein adsorption, whereas OEG-modified silver substrates show attraction and no resistance to protein adsorption.[45,46] The simulation of Ref. 44 predicted a density reduction of the water between the SAMs and, contrary to the experiments, attraction for both Au- and Ag-supported SAMs. However, the monolayers showed considerable differences in the molecular conformation on the

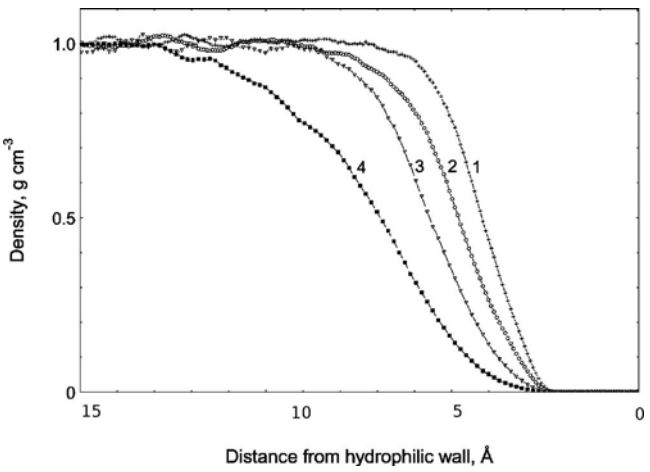

FIG. 3. Hydrophobic edges of the density profiles for water confined in an asymmetric slitlike nanopore (i.e., formed by a hydrophilic and a hydrophobic surface) as a function of the excess chemical potential μ''. Curves 1–4 are for $\mu''=-6.0$, -6.05, -6.09, and -6.095 kcal mol^{-1}, respectively. The figure is reproduced with permission from Ref. 42.

substrates due to the difference in their areal density. Silver-supported monolayers have a high area density and are impermeable to the solvent, whereas on gold, the molecules adsorb with a lower surface density that allows the solvent to penetrate into the film. This causes a disordered transition that partially changes the helical conformation into an all-trans structure. The difference between the interaction experimentally measured for the Au-supported monolayers and that predicted by the simulation was attributed to the effect of ion inclusion in the SAMs that can penetrate into the film due to the lower areal density. In real experiments, part of water dissociates into hydroxide, OH^-, and hydronium, H_3O^+. The preferential adsorption of OH^- over H_3O^+ causes a repulsion between the SAM surfaces. This effect is not seen in the simulations because the water molecules were thought ideally pure and nondissociable. The liquid was free of ions and the surface remained electrically neutral. Consequently, the interaction was dominated by the hydrophobic attraction.

In the next section, we will discuss experimental results on the density of water at surfaces with different surface energies. Unfortunately, a direct comparison of the experimental data with those found in simulations is not possible because the measurements and the simulations deal (in essence) with different systems: while the simulations are concerned with water confined between two parallel surfaces, the experiments deal with a single water/solid interface, which formally corresponds to infinite separation between the parallel plates. For increasing H, the combined effect of the two opposite surfaces on the confined water should decay and the interphase water density should increase, so that the measured density at a single water/solid interface surface will be less than simulated in a confined geometry.

III. EXPERIMENTAL OBSERVATIONS: NEUTRON AND X-RAY REFLECTOMETRY

X-ray and neutron reflectometry (NR)[47] allow the study of buried interfaces over length-scales ranging over several orders of magnitude with a resolution of a few tenths of nanometers (x-ray) and nanometers (NR), respectively. Conceptually, the experiments are relatively straightforward: a beam of neutrons or x-rays hits the surface of the sample at grazing angle and gets reflected. The intensity of the reflected beam is measured as a function of the angle or the wavelength. For a simple interface between two media, the radiation is fully reflected up to a critical angle and then it falls rapidly, giving rise to so-called Fresnel reflectivity. In the presence of a thin film, the reflection from subsequent interfaces produces fringes (Kiessig oscillations) that are related to the thickness and refractive index of the film. Typically, neutron and x-ray reflectometry calculation are expressed in terms of scattering-length densities (SLD), which are related to the refractive index through the following expression:

$$n^2 = 1 - \delta. \tag{4}$$

For neutrons δ is

$$\delta = \frac{\lambda^2}{2\pi}\rho_n = \frac{\lambda^2}{2\pi}\sum_i b_i n_i, \tag{5}$$

where λ is the wavelength, ρ_n is the neutron scattering-length density of the atomic species i, and n_i is its number density, whereas for x-ray

$$\delta = \frac{\lambda^2}{2\pi} r_e \rho_e, \tag{6}$$

where r_e is the classical electron radius and ρ_e is the electron density.

Contrary to the x-rays, the neutron scattering-length of the elements varies in a nonmonotonic way across the periodic table and varies from isotope to isotope. Therefore, the contrast can be changed and enhanced when an isotope of the same chemical element is used. One of the best known examples is the case of the two hydrogen isotopes ^1H and ^2D with scattering-lengths that differ in sign and magnitude. The ability, in the case of neutrons, to change the contrast by isotopic substitution provides unique means to selectively probe an interphase. Lu and Thomas[48] gave an overview of the potential of neutron reflectometry to investigate the average structure in layered systems along the surface normal where other techniques would fail due to disorder or to the intrinsic complexity of the layers that compose the system. There are, however, a number of uncertainties involved in modeling the density distribution extracted from reflectivity curves. The main difficulty is the so-called "phase problem" that arises from the fact that the reflectivity measured in an experiment is the square of its complex amplitude. Thus, all the phase information is lost and the density profiles resulting from the inversion of the reflectivity data are not unique. In order to reduce the ambiguities of the models, boundary conditions related to the physical properties of the studied system are introduced, and, in the case of neutrons, measurements are performed at different contrast. One further problem is the stability of a density model with respect to the number of boxes used in fitting the reflectivity curves. Finally, there is the effect of surface roughness that may result in an apparent density depletion due to the smearing of the excluded volume region in the liquid density profile.

In order to verify the prediction of theoretical work, several experiments were performed on different surfaces in contact with water. We discuss these experiments separately for hydrophobic and hydrophilic surfaces.

A. Hydrophobic surfaces

The first experimental evidence of a density deficit in the interface of water with a hydrophobic surfaces was reported independently by Steitz *et al.*,[49] Jensen *et al.*[50] and Schwendel *et al.*[51] The experiments were performed on three different surfaces and the quantitative determination of the depletion layer was significantly different in the three experiments.

Steitz *et al.*[49] performed NR on D_2O in contact with a deuterated polystyrene (d-PS) film. By spin coating d-PS on a silicon wafer they obtained a surface with a contact angle

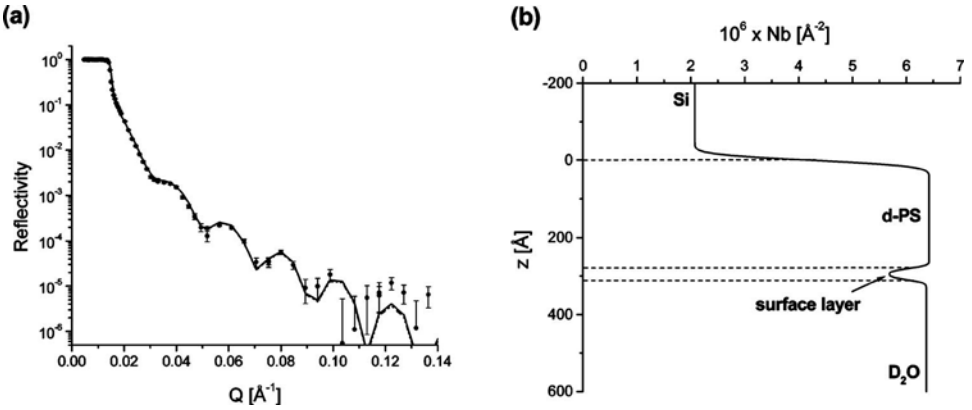

FIG. 4. Neutron reflectivity from the interface of a d-PS film (thickness=280 Å, $Nb_{dPS}=6.42\times10^{-6}$ Å^{-2}, $\sigma_{Si/dPs}=13$ Å, $\sigma_{dPS/layer}=6$ Å) between the silicon substrate and the D_2O subphase ($Nb_{D_2O}=6.37\times10^{-6}$ Å^{-2}): (a) reflectivity curve $R(Q)$; (b) scattering-length density profile ρ^s. The figure is reproduced with permission from Ref. 49.

of ~90 deg. Since the scattering-length density of d-PS is very close to that of D_2O, the reflectivity profile would be dominated by the scattering of the silicon/d-PS interface, i.e., a Fresnel reflectivity profile, if the density of the interfacial region was equal to that of the bulk phase. Their experiment instead provided evidence of a nonvanishing scattering contrast at the surface/water interface, since the reflectivity profile was characterized by a series of minima and maxima (Kiessig oscillations) due to of the interference between the neutron scattered at the silicon/polymer and polymer/D_2O interfaces. The experimental reflectivity and the scattering-length density resulting from the fit are reported in Fig. 4. The reflectivity could be fitted by including a local minimum in the scattering-length density profile at the polymer/liquid interface, which was attributed to a region of water having a reduced density. To exclude the presence of protonated contaminants, which would affect the scattering-length density in the same way a depletion layer of water would, the thickness of the deuterated PS film in air was measured prior and subsequent to the neutron-reflectometry experiment with x-rays. The invariance of the thickness was strongly indicative that the presence of protonated contaminants could be ruled out. The thickness of the depletion layer of water, d_L, was of the order of 2–5 nm, with a reduced density of ρ from 88% to 94% of the density of bulk water ρ_w (see Fig. 4). In terms of depletion distance,[37] this translates into d_2 ~0.26 nm.

Jensen *et al.*[50] probed the water interface of a paraffin monolayer (contact angle ~110 deg) floating on water by x-ray reflectometry. They found evidence of a weak dewetting (density deficit of one water molecule per 0.2 –0.25 nm^2) extending less than 1.5 nm into the bulk water, which is equivalent to a depletion distance of $d_2\sim0.1$ nm, i.e., smaller than the one predicted by Netz *et al.*[37] Schwendel *et al.*[51] measured the reflectivity profile against D_2O of self-assembled monolayers (SAMs) on gold surfaces. Nonfunctionalized hydrophobic octadecanethiolate T_m with an advancing contact angle $\theta_{adv}=115$ deg gave a reflectivity profile compatible with an extended layer of water (~5 nm) with a conspicuously reduced density. The profile could be fitted by assuming a three box model, a semi-infinite box with density of ρ_{BW} of bulk water, and two interphase layers between the bulk water and the SAMs, with different densities: a 2.1 nm layer with density $\rho=9\%\rho_{BW}$ and a 4.8 nm layer with $\rho=88\%\rho_{BW}$. This would give a depletion distance $d_2\sim2.4$ nm, which is much larger than found in simulations and other experiments. This may indicate that air inclusions in the SAM films, or surface roughness, contributed to these results. In further investigations on similar systems (dodecanethiol and hexadecanethiol monolayer adsorbed on gold) a depletion layer between 0.15 and 0.25 nm closer to the other experimental results[52] was found. The difference in the results could be also due to the presence of nanobubbles on the surface, which can form or not depending on the history of the sample, as it was proved by Zhang *et al.*[53]

We can describe the experimental results in terms of the interfacial energy of the surface with water. The interfacial energy can be expressed by $\gamma_{s,liq}=\gamma_s-\gamma_{liq}\cos\theta$, where γ_s is the surface energy of the surface, γ_{liq} is the surface tension of the liquid, and θ is the contact angle between the liquid and the surface. By using the values for the surface energies from the literature for PS,[54] paraffin,[55] and methyl-terminated alkanethiols,[56] we see that the interfacial energies between these surfaces and water are around 44, 51, and 43 mJ/m^2, which correspond to experimental depletion distances of $d_2=0.25$, 0.1, and ~0.2 nm, respectively. Although a high interfacial energy correlates with the presence of a depletion layer, there are not enough experiments to propose a dependence of depletion length on the interfacial energy. As a matter of fact, a comparison between these different experiments may be impossible because of different surface roughness and rigidity. A further complication is that the resolution of x-ray and neutron experiments is different.[57]

Among the parameters that might influence the thickness of the depletion layer are the presence of dissolved gases, temperature, pressure, chemical potential of the liquid, and *p*H. NR experiments were conducted on hexadecanethiol SAM in contact with D_2O (Ref. 52) at different temperatures between 6 and 50 °C. The results showed that the depletion

layer at 25 °C was between 2 and 2.3 nm thick with a density between 91% and 92% of the bulk water density (i.e., $d_2 = 0.16 - 0.22$ nm in terms of depletion distance), which increased with temperature, in agreement with computer simulations performed in corresponding model systems[52] and with those of Ref. 37. Experiments were also performed in the presence of two salts taken from both sides of the Hofmeister series (calcium chloride and potassium sulfate) and at two different *p*H. The depletion layer increased slightly when the two salts were added, but was left almost unaltered by *p*H.[52] By correlating these trends with how the surface energy and the free molar Gibbs energy of water are affected by temperature and dissolved salts, the results[52] could be rationalized by assuming that the extension of the depletion layer depends on at least two parameters: (i) the difference in surface energy between the solid and liquid and (ii) the temperature and solute dependent free energy of the bulk liquid-water phase, which can be estimated through the difference in the chemical potential between its vapor and liquid phase. Experiments performed on the hydrophilic SAM/cyclohexane interface (i.e., polar surface and nonpolar liquid)[52] gave a density reduction of the solvent also in this case, qualitatively correlated to the liquid/surface interfacial energy. This demonstrates that the density deficit at the solid/liquid interface is not a peculiarity of water.

The presence of dissolved gas was shown to influence the range of hydrophobic attraction between hydrophobic surfaces.[58] Dissolved gas should also accumulate between hydrophobic surfaces with obvious repercussions on the metastability of the confined fluid,[25,59] since nanoscopic "bubbles" can act as nucleation centers, providing new pathways to evaporation. The effect of the dissolved gas on the extension of the depletion layer was studied by Doshi *et al.*[60] By performing NR on quartz substrates coated with octadecyl-trichlorosilane (OTS) monolayers in contact with D_2O (Ref. 60), the depletion layer was shown to depend on the types and concentration of gasses dissolved in water. The system consisted of a layer of OTS molecules with low scattering-length density sandwiched between quartz and D_2O having a higher scattering-length density. The scattering-length density profile of the SAM was modeled with two boxes, the head group and the hydrocarbons with constant SLD and thicknesses t_{hg} and t_{hc}, respectively (Fig. 5). The depletion layer itself was modeled by a sigmoidal-error function whose midpoint was at distance δ from the hydrocarbon-water interface. With this choice, the depletion distance d_2 corresponds to $\delta/2$. For naturally aerated untreated D_2O, the depletion distance was 0.38 nm. Degassing of the liquid reduced its extension to 0.26 nm, which increased reversibly as the D_2O was placed again in contact with air for several hours. Therefore, the presence of dissolved air has the effect of increasing the extension of the depletion layer. D_2O bubbled with CO_2 and Ar resulted in depletion distances of 0.29 and 0.1 nm, respectively. No compelling explanation was given for the low value of depletion length found in the last case, but it might be dependent on the different adsorption behavior of the gasses at the

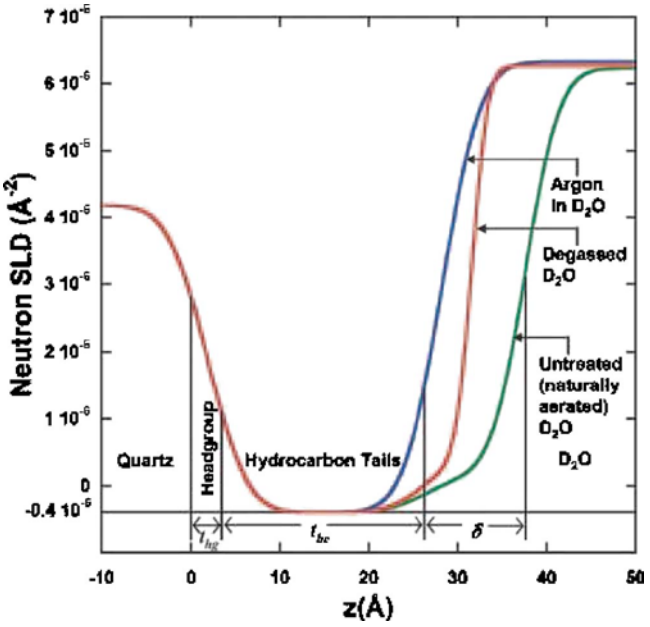

FIG. 5. The scattering-length density profile obtained from the fits of the NR measurements performed on the system quartz-OTS-D_2O for degassed and untreated water and water bubbled with argon. The OTS monolayer is modeled by two boxes, the head group and the hydrocarbons with constant SLD and thicknesses t_{hg} and t_{hc}, respectively. The density of the water in contact with the monolayer is modeled by a sigmoidal error function whose center has an offset δ from the D_2O-OTS interface. The figure is reproduced with permission from Ref. 60.

hydrophobic-water interface. The results of Doshi *et al.* are, however, in conflict with those of two x-ray reflectometry studies performed on OTS (Ref. 61) and octadecyltriethoxyloxane (OTE).[62] Both studies give evidence of water-density depletion in contact with the hydrophobic surfaces, with depletion lengths of 0.11 nm (Ref. 61) and $0 - 0.24$ nm,[62] but no dependence on the presence of gas was found.

If a vapor layer is assumed to be the origin of the density depletion, a remarkable consistency can be found between the structural data of Ref. 60 and the surface-force experiments of Ref. 63 aimed at quantifying the boundary slip effects at hydrophobic surfaces. The no-slip boundary condition of a liquid near solid surfaces does not always hold. A relevant slip occurs for water at hydrophobic surfaces. When a vapor layer of thickness d is assumed to be in contact with the hydrophobic surface, the slip can be quantified by the slip-length $b \approx d(\eta_w/\eta_v - 1)$, where η_w and η_v are the viscosities of water and vapor, respectively. The estimated value of b resulted to be 25 nm, which is not very different from the value obtained with surface-force experiments on OTS-coated Pyrex,[63] considering that two very different experimental techniques were used. Indeed, the idea that the density depletion is a vapor phase in contact with the hydrophobic surface is gaining consensus. Theory[25] seems to converge to this view. Also, the scattering experiments reported above have been explained according to this interpretation.[49,60]

Surface-force experiments aimed at measuring the dynamical shear response of water confined within asymmetric

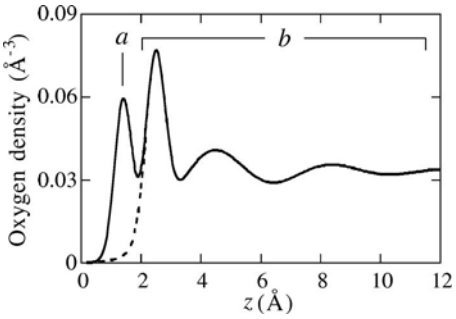

FIG. 6. The density distribution of interfacial-water oxygens as a function of distance z from the mean surface-oxygen position, obtained by x-ray reflectometry on water in contact with mica surfaces: (a) adsorbed water and (b) hydration water. The large-z-limit value of 0.033 atoms Å^3 corresponds to the mean oxygen density of bulk water. The figure is reproduced with permission from Ref. 65.

slits were also rationalized by assuming a wandering interface between a wetting-liquid phase in contact with the hydrophilic surface and a nonwetting-vapor phase in contact with the hydrophobic surface.[43] The wandering interface was characterized by a very noisy shear-response with a broad distribution of relaxation times compatible with the presence of the vapor layer in accord with grand-canonical Monte Carlo simulations.[42] An alternative way to explain a reduced density at the interface would be to hypothesize the presence of a highly structured icelike phase. However, this would be in contrast with the low viscosity found in water confined between hydrophobic surfaces.[64]

B. Hydrophilic surfaces

Contrary to hydrophobic surfaces, hydrophilic surfaces are, in principle, able to form hydrogen bonds with the water molecules in contact with them. The balance between the hydrogen bonds linking the liquid molecules and those that coordinate the water molecules to the binding site of the surface govern the conformation and the density of the liquid at the interface. Oscillating-density profiles of water molecules in the presence of a flat hydrophilic surface are predicted by computer simulations (see, for example, Ref. 42). In practice, its experimental determination is extremely complex because the hydrating molecules interact quite strongly with the surface and their molecular ordering can be smeared out by the chemical and geometrical heterogeneity of the surface. Only recently has direct evidence of density oscillation at the solid-ambient water interface been reported by Cheng *et al.*[65] in the case of water in contact with ultra-flat mica surfaces. By means of high resolution specular x-ray reflectivity, the interfacial distribution of oxygen atoms of water was determined: a first adsorbed layer was found, followed by a series of dumped hydration layers (see Fig. 6) starting at 0.25 nm above the surface. It must be noted that previous evidence of water oscillating-density was observed only under confinement between solid surfaces[66] or in the presence of applied electric fields.[67] The density of the water molecules hydrating the surface (which correspond to the combined density of the first two layers depicted in Fig. 6) resembles the density of bulk water, i.e., the presence of the surfaces does not significantly affect the hydrogen bonding between the water molecules. A negligible effect on the density in the presence of hydrophilic surfaces follows also from x-ray reflectometry experiment performed on soft hydrophilic organic monolayer layers [1-triacontanol ($C_{30}H_{61}OH$), fatty acid, monopalmitoyl glycerol ester, and dipalmitoyl glycerol ester] in contact with water having a contact angle smaller than 20 deg (Ref. 50) and tripalmitoyl glycerol ester monolayers on water with a contact angle of 70 deg.[50] For a hydroxy-terminated undecylthiolate SAM ($C_{11}OH$) (contact angle of $\theta_{adv}=20$ deg), the reflectivity profile could not be uniquely modeled: both a model with reduced density (2.25 nm layer with $\rho=60\%\rho_{BW}$ plus a 4.3 nm thick layer with $\rho=90.6\%\rho_{BW}$) and a model with increased density (10 nm layer with $\rho=108\%\rho_{BW}$ plus a 4.4 nm thick layer with $\rho=103.3\%\rho_{BW}$) provided good agreement with the experimental data, demonstrating the ambiguity and model dependence in the analysis of reflectivity data.[51]

An increased density of water in contact with an amorphous SiO_2 surface was measured by x-ray reflectivity in the quasiliquid layer resulting from the surface-melting of ice that occurs at a temperature typically 15 K below the bulk-melting temperature T_m.[68] Similar to the experiment of Steitz *et al.*,[49] the interference pattern coming from multiple interphases could be used to detect and quantify the quasi-liquid layer sandwiched between the silica substrate and the ice. For temperatures smaller than $T_0=T_m-17$ K, only a single interface between the ice and the silica was present that generated the characteristic Fresnel reflection. For temperatures higher than T_0, the multiple reflection generated at the silica–liquid-ice interface generated fringes of a period $2\pi/L$, where L is the thickness of the melted layer. The thickness and the density of this layer could be determined from the analysis of the reflectivity data. The density was significantly higher compared to bulk water: about 1.2 g/cm^3 and converged to 1.0 g/cm^3 for $T\rightarrow T_m$. The thickness increased as the temperature approached T_m, following a logarithmic growth behavior.

IV. SUM FREQUENCY GENERATION EXPERIMENTS ON THE INTERACTION OF WATER WITH NON-IONIC SURFACES

Sum frequency generation (SFG) spectroscopy is a second-order nonlinear optical technique. A visible laser beam of frequency ω_{vis} and a infra-red laser beam of tunable frequency ω_{ir} overlap at the interface and generate an output beam at the sum frequency $\omega_{sf}=\omega_{vis}+\omega_{ir}$. If the frequency range of the IR beam overlaps with the frequencies of the vibrational modes of the molecules present in the interface, SFG can be used to selectively probe these vibrations. Within the electric dipole approximation, SFG is forbidden in a centrosymmetric bulk medium, but is allowed when inversion symmetry is broken. This implies that contributions to the spectra due to isotropic bulk phases are absent and only the interfacial signal is detected. Comprehensive reviews of the use of SFG to study polymer surfaces and aqueous surfaces

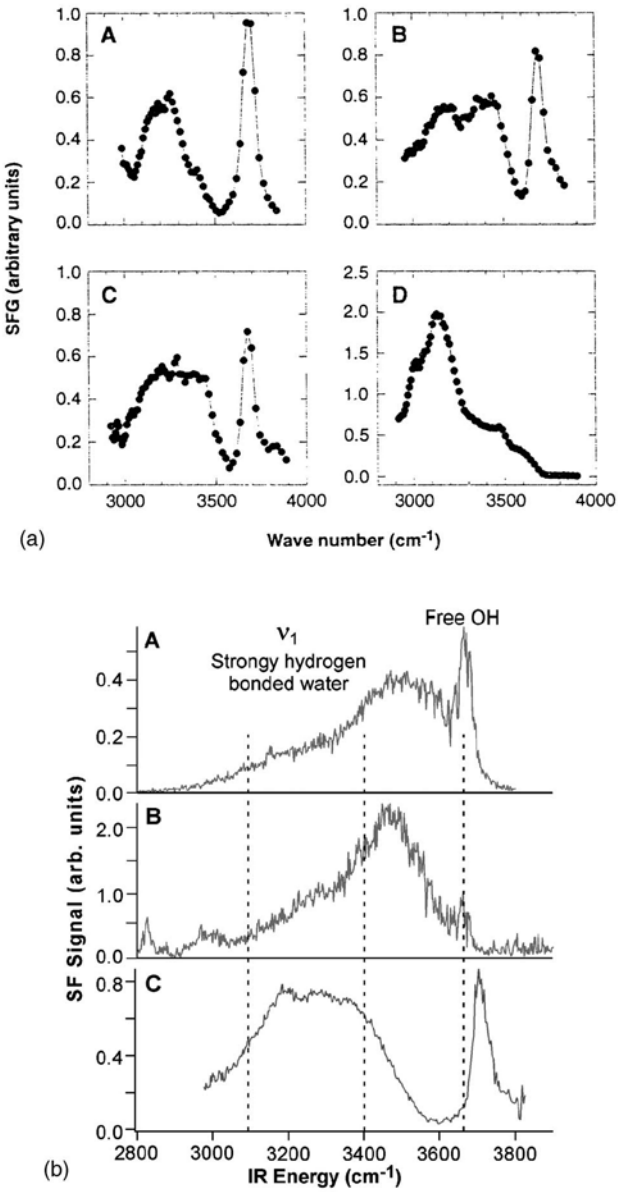

FIG. 7. (a) SFG spectra taken from Ref. 71 of the quartz-OTS water interface (A), the air-water interface (B), the hexane-water interface (C), and the quartz-ice interface (taken at 232 K)(D). (b) SFG spectra taken from Ref. 73 of the CCl_4/water (A), hexane/water (B), and vapor/water interfaces (C), indicating the difference in hydrogen bonding at the various interfaces.

have been published by Chen[69] and Richmond,[70] respectively. The vibrational spectrum of the water molecules in the range of 3000 to 3800 cm^{-1} is particularly sensitive to the local molecular environment and can be used to probe the structure of the H-bond network. However, the high sensitivity of this spectral region is accompanied by a high complexity because the different local environments in which water molecules can be found cause the vibrational resonances to widen and overlap over large frequency ranges. In addition, the coherent nature of SFG can cause complex interference patterns that make the analysis even more difficult.

In order to discuss the spectral SFG vibrational features, we reproduce in Fig. 7(a) (inset B and D) the SFG spectrum of the water/air interface and of the quartz/ice interfaces by Du *et al.*[71] Differences between these two spectra are evident over the entire energy range, reflecting different structural properties of the two systems. The spectrum of the ice/quartz interface is dominated by a pronounced peak at about 3200 cm^{-1}, which resembles the Raman OH stretch of ice.[72] At around 3400 cm^{-1}, a peak can be seen in the water/vapor spectrum that is absent in the quartz/ice. In the region around 3700 cm^{-1} a sharp peak appears in the water/vapor interface.

Of the spectral regions described above, only the last one at around 3700 cm^{-1} is assigned undoubtedly to the dangling OH bonds of the water molecules pointing into the vapor phase. This peak is indicative of a lack of H-bonding interaction and, as we will see, is typically found in hydrophobic surfaces in contact with water. The assignment of the other two peaks is still debated. In some references[71,73,74] the peak at 3200 cm^{-1} is attributed to the coupled symmetric OH stretch of water molecules tetrahedrally coordinated, i.e., to an H-bond network with a ordered icelike structure; and the peak at 3400 cm^{-1} is assigned to the H-bond of asymmetrically bonded water molecules or to water molecules with bifurcated H-bonds,[71] indicative of a waterlike disordered H-bond network. Other authors proposed that contributions to the 3400 cm^{-1} band comes mainly from water molecules directly adjacent to the surface and that the peak at 3200 cm^{-1} comes from water molecules in following water layers.[75] More recently, Buch[76] presented molecular dynamics simulations where the effect of intermolecular coupling on the OH-stretch vibrations are included. The peak at 3400 cm^{-1} was assigned to four-coordinated molecules, and the 3200 cm^{-1} to collective excitation of intermolecularly coupled H-bond vibrations. Further work of the same author, which partially revises and further elaborates these assignments, is in progress.[77] It is evident that the assignments of the two SFG peaks at lower energy (3200 and 3400 cm^{-1}) are still debated, and, with this in mind, we will review the experimental SFG results in the next sections, separately for hydrophobic and hydrophilic surfaces.

A. Hydrophobic surfaces

SFG measurements were performed on hydrophobic solid/water interfaces[71] [formed by the adsorption of OTS ($CH_3(CH_2)_{17}SiCl_3$) self assembling monolayers on fused quartz] and on the liquid/liquid water/hexane interface. The spectra [see Fig. 7(a), inset A] shows the characteristic peaks at 3200 and at 3400 cm^{-1}. The presence of a pronounced peak at 3680 cm^{-1} was also detected. That, as we have already seen for the water/air interface, is typical of surfaces unable of forming H-bonds in contact with water. This is supposedly caused by the free OH bonds of water molecules pointing toward the surface. By comparing the spectra from the solid OTS/water interface with those of the nonrigid hexane/water and air/water interfaces [Fig. 7(a), insets A and C], the peak at 3400 cm^{-1} is more relevant for the latter. These results suggest that the rigidity of the constraint affects the SFG features, i.e., the connectivity and the orientation of the hydrogen bonding at the interface. Du *et al.*[71] assign the

peaks at 3200 and 3400 cm^{-1} to icelike ordered and disordered liquidlike water molecules, respectively. According to the authors of Ref. 71 the higher degree of orientation occurring on solid surfaces could be explained by the necessity to compensate the H-bonds that cannot be formed with the nonpolar surface; in order to maximize their number (or to minimize the number of lost H-bonds), the interfacial water molecules try to adopt a hexagonal structure, in which one fourth of them have dangling OH-bonds pointing toward the hydrophobic surface. This interpretation is, however, speculative and in contrast with the low viscosity found in water confined between hydrophobic surfaces;[43,64] a thin layer of highly oriented water would behave in a solidlike fashion and would be characterized by a higher value of viscosity. Instead, there is experimental evidence that water confined in sub-nanometric environments, unlike nonassociative liquids, maintains a viscosity typical of bulk liquid.[64,78]

Further SFG studies were made on CCl_4/water and hydrocarbon/water by Scatena *et al.*[73] The wide range of spectral contributions of the systems was discussed[79] and it was shown (see below) that significant information on the structure of the hydrogen-bond network at the water interfaces could be obtained by combining frequency and orientational information coming from SFG spectra. By comparing the spectra of CCl_4/water and hydrocarbon/water interfaces with that of the vapor/water interface [see Fig. 7(b)], they noted that the spectra were dominated by the higher-energy peaks (3400 and 3669 cm^{-1}) and observed a drop of intensities in the peaks at lower energies (3200 cm^{-1}). Their fits were improved by adding, besides the three peaks at 3200, 3400, and 3700 cm^{-1}, additional ones corresponding to other water interfacial species. In particular they supposed that a part of the water molecules present at the hydrophobic liquid/water interface have weak or negligible H-bond interaction with other interfacial water molecules. Part of these molecules are composed by water monomers in the organic phase (whose H atoms are pointed toward it) with an absent or negligible interaction with other water molecules. Another part is composed of H-bond acceptor water molecules partially immersed in the organic phase, having their H atoms pointing toward it and with an orientation sensitive to *p*H variation.

B. Hydrophilic surfaces

In contrast to hydrophobic surfaces, the SFG spectra obtained for water in contact with hydrophilic surfaces are characterized by the lack of the spectral contribution from the free OH-bonds at 3700 cm^{-1}. Since these surfaces can interact with the water molecules through H-bonds, the dangling H-bonds oriented towards the surface are absent. SFG spectra were measured at the interface between water and three different hydrophilic solids, SiO_2,[74] TiO_2,[80] and CaF_2.[81] In all these studies, the *p*H was varied to see the effect of the surface charge on the molecular orientation. Du *et al.* studied the OH stretch vibration of water molecules at hydrophilic fused-quartz surfaces.[74] They found that the interfacial orientation and bonding of water molecules are strongly affected by (i) electrostatic interactions with the surface charges induced by ionization of the SiOH groups and (ii) hydrogen bonding of the molecules with SiOH groups. The two interactions have the opposite effect. By varying the *p*H of the bulk water, and consequently the degree of surface ionization, they could change the relative contribution of each of the two interactions. For highly ionized surfaces (high *p*H), several monolayers of water can be oriented by the intense electric field, with their dipoles pointing toward the surface. The degree of orientational order was identified by following the intensity of the peaks at 3200 and 3400 cm^{-1} (see Fig. 8). At low *p*H, the surface is uncharged and the interfacial water tends to form H-bonds with the O atom facing the quartz surface, i.e., opposite to the orientation observed at high *p*H. Orientational order extends only over one or two layers of interfacial water, giving peaks with lower intensity. In the intermediate *p*H range (partially ionized surface), the interfacial water was characterized by a lower degree of order due to the competition between hydrogen bonding with the surface-silanol group and the orientation induced by the surface field. The experiments showed that the surface charge following the changes in *p*H can induce a flip in the molecular orientation. Note that neutron reflectometry experiments did not show detectable effects on the density at the solid/water interface caused by changes in *p*H.[52]

Compared to SiO_2, the TiO_2/water interface has richer spectroscopic features because the isoelectric point (the *p*H at which the surface has a neutral charge) is at *p*H 5.5, in contrast to *p*H 2 for SiO_2. By performing measurements at different *p*H, the effect of changing the surface charge from negative to positive values was evaluated by Kataoka *et al.*[80] The characteristic spectral features at 3200 cm^{-1} and at 3400 cm^{-1} were followed by varying *p*H. It was shown that both peaks displayed a minimum at the isoelectric point for TiO_2. The intensity of the 3200 cm^{-1} peak increased significantly both at lower or at higher *p*H, which means that a charged surface induces molecular orientation of the water molecules. By adding phosphate anions to the solution, which adsorb quite strongly to the surface, Kataoka *et al.* could shift the isoelectric point of the surface to resemble that of a SiO_2 surface (*p*H 2). In this case, the intensity of the peak at 3200 cm^{-1} as a function of *p*H was very similar to that of the SiO_2, i.e., a monotonic increase with *p*H.

SFG experiments were also performed at the CaF_2/water interface.[81] At low *p*H, the spectrum was dominated by the peak at 3200 cm^{-1} due to the orientation of water molecules, with a small contribution also in the 3400 cm^{-1} region. At the isoelectric point (around *p*H 6.4), the sum frequency response falls to zero, indicating a full randomization of the water molecules at the interface. At $pH > 6.4$, the contribution at 3200 cm^{-1} reappears, although in minor proportion, along with a peak at 3675 cm^{-1}. This peak was assigned to weakly hydrogen bonded Ca-OH groups originated at high *p*H from ion exchange of surface fluorine and free OH^-, or from specific adsorption of OH^- groups from solution.[82] All

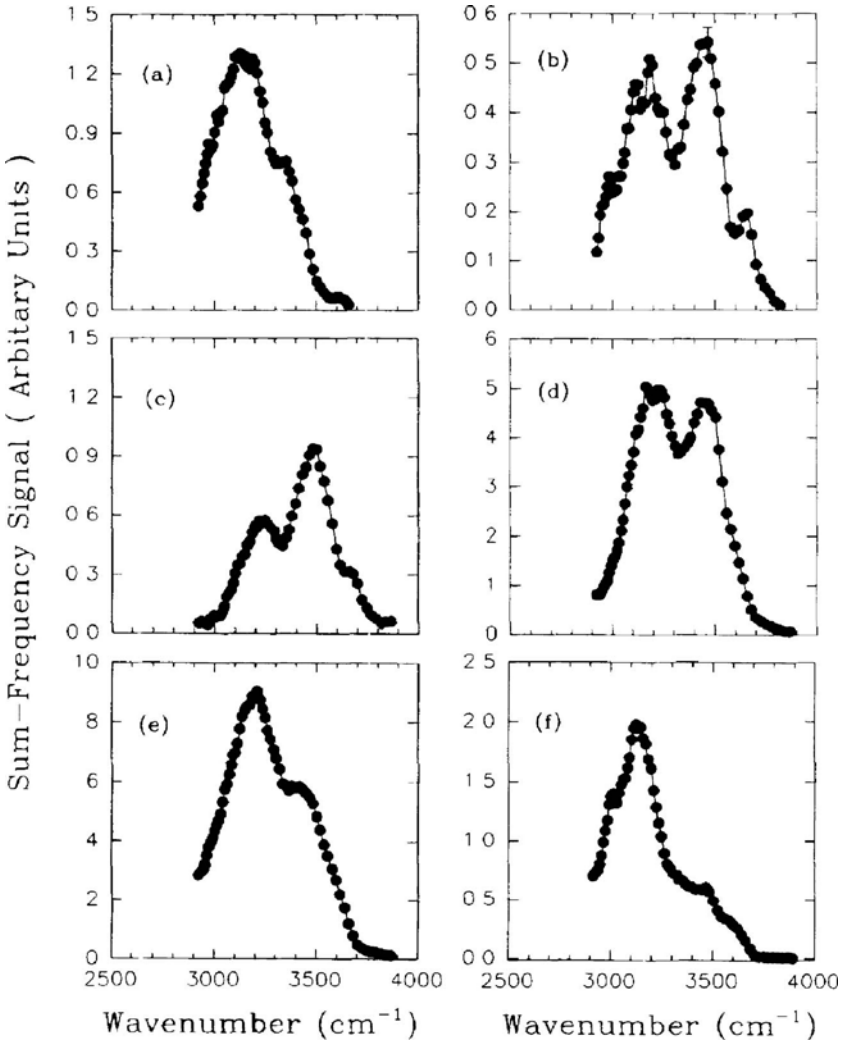

FIG. 8. SFG spectra from the quartz/water interface with different *p*H values in the bulk water. (a) *p*H=1.5; (b) *p*H=3.8; (c) *p*H=5.6; (d) *p*H=8.0; (e) *p*H=12.3; (f) SFG spectrum from the quartz/ice interface. The figure is reproduced with permission from Ref. 74.

the experiments above show evidence of the role of the surface charge in determining the orientation of water molecules at the hydrophilic interface.

Kim *et al.*[83] studied the structure of the interfacial water at the solid/liquid interface in the presence of supported lipid bilayers (SLB), which provide a 0.5 to 1.5 nm confinement[83] to the water molecule sandwiched between the quartz and the bilayer. The intensity of the peaks and the oscillator strength was followed for the bare quartz interfaces and various neutral, positive, and negative charged bilayers by varying the *p*H and the electrolyte concentration. They found that, although the trends of the measured quantities for the various bilayers as the *p*H is varied are similar to each other, the intensities of the 3400 cm^{-1} peaks were reduced in the presence of positively charged and neutral supported lipid bilayers and increased in the presence of negative SLB. On the contrary, the intensities of the 3200 cm^{-1} peaks increased for positively charged SLB and decreased in the presence of negatively charged SLB. In cellular environments, a high number of complex supramolecular structure, like membranes and proteins, interact with each other in environments where tight confinement is the normal condition. The interaction between them responds dramatically to subtle change in the aqueous medium where the system is immersed. Performing experiments in confined geometry on simpler model systems (like lipid bilayers) can help increase understanding of a wide range of phenomena occurring in complex biological systems that so far have been very difficult to rationalize.

V. SUMMARY AND CONCLUSIONS

In the previous sections, we reviewed the results obtained by computer simulations, neutron and x-ray reflectometry, and sum frequency generation spectroscopy on water interfaces. These methods measure different structural aspects of water/solid interfaces. Computer simulations can describe the system with molecular resolution and thus help us to understand what particular properties of the water/water and water/surface potentials are responsible for the sign and magnitude of the hydration force, which can be studied in its pure form aside from the contributions of other forces between the confining surfaces (e.g., electrostatic, van der Waals). Moreover, these methods have the advantage that the interaction between model surfaces free of imperfections can be studied. However, the cooperative nature of hydrogen bonding can be represented only in an effective way by the

two-body potentials generally used. Only recently have potentials that can describe explicitly many-body water potential appeared in computer simulations.[30]

Neutron and x-ray reflectometry can explore the density of water orthogonal to the interface with different resolution, higher for x-ray. Neutron reflectometry has the possibility to use contrast variation to enhance its performance.

SFG spectroscopy can probe the vibrational spectra of the water molecules at the interface. The OH stretching vibrations are extremely sensitive to the local environment. This high sensitivity is accompanied by complexity in the SFG spectra, thus their interpretation is difficult and still an issue of discussion.

Hydrophobic surfaces in contact with water are characterized by some distinct features: theory predicts that the region in direct contact with the hydrophobic surface is less stable than the liquid phase[25] and simulations[37,42] accordingly envisage a thin layer of water with low density, although thinner than what was predicted by theory.[25] The density depletion was experimentally confirmed by neutron and x-ray reflectometry[49–52] and is ascribed to the presence of a layer of water with reduced density or a vapor layer at the solid/liquid interface. Significant differences were found in the reported extensions of the depletion layer, although a direct comparison between these interfaces cannot be easily done in view of the different surfaces used. The SFG spectra in the region of 2800 to 3800 cm^{-1} corresponds to the OH stretching modes, which are extremely sensitive to hydrogen-bonding interactions between the water molecules. Hydrophobicity manifests itself with the appearance of a distinct peak around 3700 cm^{-1}, which corresponds to a free OH group that cannot form a hydrogen bond with the nonpolar surface. The spectral region around 3200 cm^{-1} is typically assigned to OH groups in a tetrahedral H-bond environment, whereas peaks at 3400 cm^{-1} are associated with the OH groups that participate in disordered H-bonds. However, contrary to these assignments, other representations have been proposed in the literature: the peaks at 3400 and 3200 cm^{-1} were assigned to water molecules adjacent to the surface and in the following water layer, respectively.[75] Alternatively, the two peaks were assigned to four-coordinated molecules and collective excitation of intermolecularly coupled H-bonds, respectively.[76]

Experiments performed on water in contact with organic liquid phases[73] and rigid[71] surfaces show that the kind of constraint imposed by the confining surface affects the water connectivity via H-bonds. In one study,[71] the low water density found at the hydrophobic surface was explained by assuming that the water is in a low-density icelike structure. This interpretation, motivated by the increase of the SFG peak at 3200 cm^{-1} (supposedly indicative of enhanced organization of the H-bond), is, however, speculative and is not supported by the results found with surface-force experiments. Although SFG and surface-force measurements are performed on different systems (semi-infinite water at a hydrophobic surface and water confined in a slitlike nanopore formed by hydrophobic surfaces), it would be difficult to explain the low viscosity found in shear force experiments of water confined between hydrophobic surfaces[64] with a highly organized icelike water layer.

Hydrophilic surfaces in contact with water present substantially different features. Evidence for hard wall density oscillations were found,[65] and the average density at the interface was comparable to the bulk density.[50,65] However, the results of one neutron reflectometry experiment[51] gave equal probability of an increased and depleted density. Evidence of density depletion was found for hydrophilic surfaces in contact with a nonpolar solvent.[52] This experiment is very important because it shows that the solvophobic density depletion is not specific to water, but is more general and correlated with the interfacial energy of the liquid with the solid surface. More experiments should be performed in this direction (e.g., analyzing the trend in temperature) in order to establish to what extent water behaves differently from other liquids.

Surprisingly, the neutron (x-ray) scattering and sum frequency generation spectroscopy communities have not interacted substantially, despite the fact that parallel studies performed with these techniques could help in understanding water interfaces. In order to have meaningful complementary information, SFG and scattering experiments should be performed on interfaces prepared identically, because the hydration of solid surfaces depends in a complex way on the physical and chemical properties of the surfaces used.[12] Roughness, surface energy, number, and rigidity of the surface group that can form H-bonds can all contribute in a way that is not completely known. To understand how the various properties of the surface affect density depletion and the orientation of the water molecules, experiments should be performed by changing only one parameter at a time. This could be achieved by performing NR measurement on surfaces formed from mixed self-assembled monolayers with different hydrophilic and hydrophobic surface groups.[84] By appropriate mixing of the two components, the surface tension of the resulting surfaces could be changed at a constant thickness and roughness. The chemical composition of the surface can also be changed with respect to the relative amount of H-bond donors or acceptors. Amino- and carboxylic-acid-terminated SAMs could be used to form surfaces that can induce only density variation (carrying an equal amount of hydrogen bond donors and acceptors) or will induce both density and orientational change (possessing, for example, only hydrogen bond donors). By using SAMs with different chain length, the roughness can be varied at a constant chemical composition to verify the dependence of the depletion layer on this property of the system. By controlling the surface properties, whether a lower limit of hydrophobicity (as measured by the contact angle or surface energy) of the surface exists in order to have a depletion layer could be studied.

In view of the important role that hydrophobic forces play in biological and colloidal science, it is interesting to evaluate possible correlations between the structural studies of water at the hydrophobic interface with direct measurements of

forces between hydrophobic surfaces in water. As stated in the Introduction, a review of the surface-force experiments is outside the scope of this article, also in view of the fact that many surface-force measurements show contradictory results that are difficult to rationalize.[12] Here we will describe one significant result. The experiments in Ref. 52, on the density depletion at the interface between water and hexadecanethiol modified gold substrate, fit well the surface-force experiment of Ref. 85 performed on very similar surfaces. The last point is important because experiments performed on surfaces obtained by different methods of preparation exhibit significantly different ranges and magnitudes of the forces,[12] even when macroscopic properties such as the contact angles are the same. The surface-force experiments show no interaction as long as the surfaces are at a distance larger than several nanometers until they jump into contact. The jump-in distance is around 5 nm in pure water at room temperature. This is fairly close to twice the extension of the depletion layer measured in Ref. 52 at room temperature. The strong attraction seems to occur when the interfacial low-density regions of water adjacent to each surface overlap. Also, the effect of salts seemed compatible in the two experiments, because both the extension of the depletion layer and the jump-in distance increased in the presence of salts. Even though a comparison can only be qualitative since the jump-in distance in the AFM experiment depends on the spring constant of the cantilever used, the correlation of the trend observed in the presence of salts is still very remarkable. This comparative analysis between the density of water in proximity of a surface and the water-mediated interactions between the surfaces should be extended to other surfaces commonly used in surface-force studies. As pointed out by Israelachvili one decade ago, it is not clear if the peculiarities of the water mediated interactions have more to do with intrinsic properties of water or, rather, with the physical and chemical properties of the surfaces.[2] A definitive answer to this question has not yet been given, and greater effort should be made in this direction.

ACKNOWLEDGMENTS

Professor M. Grunze is gratefully acknowledged for fundamental advice and suggestions on how to organize the present work. Professor A. J. Pertsin, Dr. M Himmelhaus, Dr. R. Steitz, Professor R. Netz, Professor E. Kokkoli, Dr. J. Fick, Professor V. Buch, and Professor Y. R. Shen are acknowledged for the useful discussions. We acknowledge the financial support of Helmholtz Association of National Research Centres (HGF), within the framework of the Virtuelle Institut Funktionelle Eigenschaften Aquatischer Grenzflaechen Bonn, Germany, the EU Strep Nanocues, and Office of Naval Research.

[1]R. Evans and U. M. B. Marconi, J. Chem. Phys. **86**, 7138 (1987).
[2]J. Israelachvili and H. Wennerström, Nature (London) **379**, 219 (1996).
[3]S. Dietrich, J. Phys.: Condens. Matter **8**, 9127 (1996).
[4]R. Evans, R. J. F. Leote de Carvalho, J. R. Henderson, and D. C. Hoyle, J. Phys. Chem. **100**, 591 (1994).
[5]B. Bhushan, J. N. Israelachvili, and U. Landman, Nature (London) **374**, 607 (1995).
[6]J. Gao, W. D. Leudtke, and U. Landman, Phys. Rev. Lett. **79**, 705 (1997).
[7]J. E. Curry, J. Chem. Phys. **113**, 2400 (2000).
[8]S. T. Cui, P. T. Cummings, and H. D. Cochran, J. Chem. Phys. **114**, 7189 (2001).
[9]S. H. Lee and P. J. Rossky, J. Chem. Phys. **100**, 3334 (1994).
[10]T. Hayashi, A. J. Pertsin, and M. Grunze, J. Chem. Phys. **117**, 6271 (2002).
[11]D. Leckband and J. Iraelachivili, Q. Rev. Biophys. **34**, 105 (2001).
[12]H. K. Christenson and P. M. Claesson, Adv. Colloid Interface Sci. **91**, 391 (2001).
[13]J. Milhaud, Biochim. Biophys. Acta **1663**, 19 (2004).
[14]L. R. Pratt and A. Pohorille, Chem. Rev. **102**, 2671 (2002).
[15]K. Murzyn, W. Zhao, M. Karttunen, M. Kurdziel, and T. Rog, Biointerphases **1**, 98 (2006).
[16]K. Aman, E. Lindahl, O. Edholm, P. Hakansson, and P.-O. Westlund, Biophys. J. **84**, 115 (2003).
[17]S. E. Feller, A. Rojunkarin, S. Bogusz, and B. R. Brooks, J. Phys. Chem. **100**, 17011 (1996).
[18]E. A. Vogler, Adv. Colloid Interface Sci. **74**, 69 (1998).
[19]D. Quere, Physica A **313**, 32 (2002).
[20]R. E. Johnson and R. H. Dettre, Adv. Chem. Ser. **43**, 112 (1964).
[21]P. G. De Gennes, Rev. Mod. Phys. **57**(3), 827 (1985).
[22]G. Ash, D. H. Everett, and C. Radke, J. Chem. Soc., Faraday Trans. 2 **69**, 1256 (1973).
[23]D. G. Hall, J. Chem. Soc., Faraday Trans. 2 **68**, 2169 (1972).
[24]P. Attard, D. R. Berard, C. P. Ursenbach, and G. N. Patey, Phys. Rev. A **44**, 8224 (1991).
[25]K. Lum, D. Chandler, and J. D. Weeks, J. Phys. Chem. B **103**, 4570 (1999).
[26]N. A. M. Besseling, Langmuir **13**, 2113 (1997).
[27]J. J. Magda, M. Tirrel, and H. T. Davis, J. Chem. Phys. **83**, 1888 (1985).
[28]J. Gao, W. D. Luedtke, and U. Landman, J. Phys. Chem. B **102**, 5033 (1998).
[29]V. Buch and J. P. Devlin, *Water in Confined Geometries* (Springer, Berlin, 2003).
[30]W. L. Jorgensen and J. Tirado-Rives, Proc. Natl. Acad. Sci. U.S.A. **102**, 6665 (2005).
[31]A. Wallqvist and B. J. Berne, J. Phys. Chem. **99**, 2893 (1995).
[32]A. Wallqvist and B. J. Berne, J. Phys. Chem. **97**, 13841 (1993).
[33]J. Forsman, B. Joensson, and C. E. Woodward, J. Phys. Chem. **100**, 15005 (1996).
[34]J. P. Postma, H. J. C. Berendsen, and J. R. Haak, Faraday Symp. Chem. Soc. **17**, 55 (1982).
[35]W. L. Jorgensen, J. Chandrasekhar, J. D. Madura, R. W. Impey, and M. L. Klein, J. Chem. Phys. **79**, 926 (1983).
[36]J. Forsman, C. E. Woodward, and B. Joensson, Langmuir **13**, 5459 (1997).
[37]S. I. Mamatkulov, P. K. Khabibullaev, and R. R. Netz, Langmuir **20**, 4756 (2004).
[38]A. Pertsin and M. Grunze, J. Phys. Chem. B **108**, 1357 (2004).
[39]G. Hummer, J. C. Rasaiah, and J. P. Noworyta, Nature (London) **414**, 188 (2001).
[40]K. Koga, G. T. Gao, H. Tanaka, and X. C. Zeng, Nature (London) **412**, 802 (2001).
[41]W. H. Noon, K. D. Ausman, R. E. Smalley, and J. Ma, Chem. Phys. Lett. **355**, 445 (2002).
[42]A. Pertsin and M. Grunze, J. Phys. Chem. B **108**, 16533 (2004).
[43]X. Zhang, Y. Zhu, and S. Granick, Science **295**, 663 (2002).
[44]A. J. Pertsin, T. Hayashi, and M. Grunze, J. Phys. Chem. **106**, 12274 (2002).
[45]C. Dicke, K. Feldman, W. Eck, S. Herrwerth, and G. Häner, Polym. Prepr. (Am. Chem. Soc. Div. Polym. Chem.) **41**, 1444 (2001).
[46]P. Harder, M. Grunze, R. Dahint, G. M. Whitesedes, and P. E. Labinis, J. Phys. Chem. B **102**, 426 (1998).
[47]J. Daillant and A. Gibauds, in *X-ray and Neutron Reflectivity: Principles and Applications* (Springer, Berlin, 1999).
[48]J. R. Lu and R. K. Thomas, J. Chem. Soc., Faraday Trans. **94**, 995 (1998).
[49]R. Steitz, T. Gutberlet, T. Hauss, B. Klosgen, R. Krastev, S. Schemmel, A. C. Simonsen, and G. H. Findenegg, Langmuir **19**, 2409 (2003).
[50]T. R. Jensen, M. O. Jensen, N. Reitzel, K. Balashev, G. H. Peters, K. Kajer, and T. Bjornholm, Phys. Rev. Lett. **90**, 086101 (2003).

[51]D. Schwendel, T. Hayashi, R. Dahint, A. Pertsin, M. Grunze, R. Steitz, and F. Schreiber, Langmuir **19**, 2284 (2003).
[52]M. Maccarini, R. Steitz, M. Himmelhaus, J. Fick, S. Tatur, M. Grunze, J. Janecek, and R. R. Netz, Langmuir **23**, 598 (2007).
[53]X. H. Zhang, A. Khan, and W. A. Ducker, Phys. Rev. Lett. **98**, 136101 (2007).
[54]D. K. Owens, J. Appl. Polym. Sci. **13**, 1741 (1969).
[55]J. Israelachvili, *Intermolecular and Surface Forces* (Academic, London, 1992).
[56]V. I. Silin, H. Wieder, J. T. Woodward, G. Valincius, A. Offenhausser, and A. L. Plant, J. Am. Chem. Soc. **124**, 14676 (2002).
[57]P. Ball, Nature (London) **423**, 25 (2003).
[58]E. E. Meyer, Q. Lin, and J. N. Israelachvili, Langmuir **21**, 256 (2005).
[59]K. Leung, A. Luzar, and D. Bratko, Phys. Rev. Lett. **90**, 065502 (2003).
[60]D. A. Doshi, E. B. Watkins, J. N. Israelachvili, and J. Majewski, Proc. Natl. Acad. Sci. U.S.A. **102**, 9458 (2005).
[61]M. Mezger, H. Reichert, S. Schöder, J. Okasinki, H. Schrödre, H. Dosch, D. Palms, J. Ralston, and V. Honkimäki, Proc. Natl. Acad. Sci. U.S.A. **103**, 18401 (2006).
[62]A. Poynor, L. Hong, I. K. Robinson, and S. Granick, Phys. Rev. Lett. **97**, 266101 (2006).
[63]C. Cottin-Bizonne, B. Cross, A. Steinberger, and E. Charlaix, Phys. Rev. Lett. **94**, 056102 (2005).
[64]U. Raviv, S. Gaisson, J. Frey, and J. Klein, J. Phys.: Condens. Matter **14**, 9275 (2002).
[65]L. Cheng, P. Fenter, K. L. Nagy, M. L. Schegel, and N. C. Sturchio, Phys. Rev. Lett. **87**(15), 156103 (2001).
[66]J. Wang, B. M. Ocko, A. J. Davenport, and H. S. Isaacs, Phys. Rev. B **46**, 321 (1992); M. F. Toney, J. N. Howard, J. Richer, G. L. Borges, J. G. Gordon, O. R. Melroy, D. G. Wiesler, D. Lee, and L. B. Sorensen, Nature (London) **368**, 444 (1994); Y. S. Chu, T. E. Lister, W. G. Cullen, H. You, and Z. Nagy, Phys. Rev. Lett. **86**, 3364 (2001).
[67]J. N. Israelachvili and R. M. Pashley, Nature (London) **306**, 249 (1983); J. Israelachvili and H. Wennerström, *ibid.* **379**, 219 (1996); J. P. Cleveland, T. E. Schäffer, and P. K. Hansma, Phys. Rev. B **52**, R8692 (1995).
[68]S. Engemann, H. Reichert, H. Dosch, J. Bilgram, V. Honkimäki, and A. Snigirev, Phys. Rev. Lett. **92**, 205701 (2004).
[69]Z. Chen, Y. R. Shen, and G. A. Somorjai, Annu. Rev. Phys. Chem. **53**, 437 (2002).
[70]G. L. Richmond, Annu. Rev. Phys. Chem. **52**, 357 (2001).
[71]Q. Du, E. Freysz, and Y. R. Shen, Science **264**, 826 (1994).
[72]J. R. Scherer and R. G. Snyder, J. Phys. Chem. **67**, 4794 (1977).
[73]L. F. Scatena, M. G. Brown, and G. L. Richmond, Science **292**, 908 (2001).
[74]Q. Du, E. Freysz, and Y. R. Shen, Phys. Rev. Lett. **72**, 238 (1994).
[75]M. C. Gurau, G. Kim, S. M. Lim, F. Albertorio, H. C. Fleischer, and P. Cremer, ChemPhysChem **4**, 1231 (2003).
[76]V. Buch, J. Phys. Chem. B **109**, 17771 (2005).
[77]Private communication.
[78]U. Raviv, P. Laurat, and J. Klein, Nature (London) **413**, 51 (2001).
[79]G. M. Brown, E. A. Raymond, C. H. Allen, L. F. Scatena, and G. L. Richmond, J. Phys. Chem. A **104**, 10220 (2000).
[80]S. Kataoka, M. C. Gurau, F. Albertorio, M. A. Holden, S. M. Lim, R. D. Yang, and P. Cremer, Langmuir **20**, 1662 (2004).
[81]K. A. Becraft and G. L. Richmond, Langmuir **17**, 7721 (2001).
[82]L. Wu and W. J. Forsling, J. Colloid Interface Sci. **174**, 178 (1995).
[83]J. Kim, G. Kim, and P. S. Cremer, Langmuir **17**, 7255 (2001).
[84]See, for example, C. D. Bain and G. M. Whitesides, J. Am. Chem. Soc. **110**, 6560 (1988); A. Heise, M. Stamm, M. Rauscher, H. Duschner, and H. Menzel, Thin Solid Films **327-329**, 199 (1998).
[85]E. Kokkoli and C. F. Zukoski, Langmuir **14**, 1189 (1998).